ELSEVIER

Journal of Neuroscience Methods 88 (1999) 153–161

JOURNAL OF NEUROSCIENCE METHODS

Demonstration of two distributions of vesicle radius in the dopamine neuron of *Planorbis corneus* from electrochemical data

Brian B. Anderson, Guangyao Chen, David A. Gutman, Andrew G. Ewing *

Penn State University, Department of Chemistry, 152 Davey Laboratory, University Park, PA 16802, USA

Received 28 May 1998; received in revised form 26 January 1999; accepted 30 January 1999

Abstract

An electrochemical model to calculate the relative size and neurotransmitter concentration of individual nerve cell vesicles is presented to examine potentially different types of vesicles in *Planorbis corneus*. Amperometric current transients resulting from individual exocytosis events detected from single cells contain the information necessary to quantify vesicular neurotransmitter amount and to estimate other important cellular properties such as vesicular neurotransmitter concentration and vesicle radius. Use of a simplifying assumption that the cross-sectional area of the contents of each release event is the apparent electroactive area of the electrode and that the shape of the decreasing phase of each current transient follows Cottrell-like behavior, the Cottrell equation and Faraday's law can be combined to yield expressions for relative vesicle radius and neurotransmitter concentration. This analysis has been applied to data obtained from the cell body of the giant dopamine neuron of the pond snail *P. corneus*. The histogram of vesicular dopamine concentration reveals a single wide distribution and the histogram of vesicle radius reveals a bimodal radius distribution. These data strongly suggest two distinct classes of vesicle radius in the *P. corneus* neuron lead to the bimodal distribution of amount released reported earlier.

Keywords: *Planorbis corneus*; Electrochemistry; Exocytosis; Vesicle size distribution; Vesicular neurotransmitter concentration distribution; Model of exocytosis

1. Introduction

Nerve cells release neurotransmitter substances packaged in vesicles through a process called exocytosis. Detecting the minute quantities of chemicals released from those vesicles is an analytical challenge. Since its introduction in 1990 (Leszczyszyn et al., 1990), electrochemical detection of exocytosis from single cells has, in part, met that challenge (Clark and Ewing, 1997). In a typical experiment, a microelectrode is manipulated up to a cell and then the cell is chemically or electrically stimulated to elicit exocytosis. Upon stimulation, vesicles inside the cell fuse with the cell membrane and release their contents into the extracellular fluid. Any electroactive material released from vesicles that fuses directly below the electrode is completely oxidized allowing quantitation of the contents of individual vesicles.

The first example of this type of experiment was performed by Leszczyszyn et al. (1990), where they detected stimulated release of catecholamines from bovine adrenal medullary cells. Since then, many different cell lines have been investigated. In addition to work on adrenal cells (Leszczyszyn et al., 1990, 1991; Wightman et al., 1991; Chow et al., 1992; Zhou et al., 1994), mast cells (Alvarez de Toledo et al., 1993; Pihel et al., 1995), rat pheochromocytoma (PC 12) cells (Chen et al., 1994; Zerby and Ewing, 1996), pancreatic β-cells (Kennedy et al., 1993), and superior cervical ganglion neurons (Zhou and Misler, 1995) have been studied. Electrochemical detection of exocytosis has

* Corresponding author. Tel.: +1-814-863-4563; fax: +1-814-863-8081.

E-mail address: age@psuvm.psu.edu (A.G. Ewing)

0165-0270/99/$ - see front matter
PII: S0165-0270(99)00024-2

also been applied to invertebrate neurons. The leech serotonin neuron has been studied in culture (Bruns and Jahn, 1995) and the cell body of the identified giant dopamine neuron of the freshwater pond snail *Planorbis corneus* has been studied in vivo (Chen and Ewing, 1995; Chen et al., 1995, 1996).

The earliest experiments of this type employed voltammetry as a detection scheme (Leszczyszyn et al., 1990). Constant potential electrochemistry or amperometry is most often used, however, because of its high sensitivity and fast response time. These properties allow the detection of small amounts of electroactive compounds on the microsecond time scale. Amperometry is an ideal electrochemical technique for evaluating exocytosis because vesicles may contain only a few thousand electroactive molecules and be released on a time scale of several hundred microseconds.

In addition to being fast and sensitive, amperometry yields data that are straightforward to quantify. When the electrode is held at a potential where the analyte oxidation is diffusion limited, analyte in the confined space between the cell and the electrode is quantitatively oxidized. Therefore, the amount of charge passed at the electrode surface is directly proportional to the number of moles of analyte by Faraday's law:

$$Q = nNF \quad (1)$$

where Q is the charge passed at the electrode surface, n is the number of moles of electrons transferred per mole of analyte oxidized (two for catecholamines), N is the number of moles of detected analyte, and F is the Faraday constant (96485 C/mol). By calculating N for all detected release events from many cells, a histogram of the number of moles of vesicular neurotransmitter can be calculated. Furthermore, the vesicular amount can apparently be correlated with vesicle size for each release event by plotting the frequency of release events vs. the cube root of vesicle amount (mol). Such an analysis is valid because adrenal cells (Coupland, 1968), PC-12 cells (Schubert et al., 1980) and pancreatic β-cells (Larsson et al., 1976) are known to have a Gaussian distribution of vesicle radius. Making the crude assumption that all vesicles in a given cell contain neurotransmitter at a constant concentration, the vesicular amount of neurotransmitter is proportional to the vesicle size. Therefore, the cube root histogram has a Gaussian shape that is said to reflect the vesicle size distribution. This reasoning has been extended to the GDC in *P. corneus* (Chen and Ewing, 1995; Chen et al., 1995). In this system, two distinct Gaussian distributions of neurotransmitter amount released have been reported (Chen et al., 1995). Although the cube root of vesicle amount histograms yield an approximation of the size distribution of vesicles, no information about the vesicular neurotransmitter concentration is obtained, thus it has not yet been possible to define whether the different distributions result from two populations of vesicle radius or concentration.

A probability density function can be fit to the vesicle content distribution obtained by amperometry, and can be used to calculate vesicular neurotransmitter concentration if a single distribution of vesicle radius is present, and if that distribution is known. Wightman et al. (1991) have used a probability density function for the distribution of vesicle content to calculate adrenal cell vesicular catecholamine concentration. A similar treatment has been performed on data obtained from human pancreatic β-cells and rat PC-12 cells (Finnegan et al., 1996). It is important to realize that events that occur at sites that are not directly across from the electrode are essentially undetected (Wightman et al., 1995). This is easily understood as diffusion from the release site is equal in all directions, hence, events occurring at points removed from the electrode contribute only to a broad, dilute background and not to millisecond transients.

Quantitation of vesicle radius and vesicular neurotransmitter concentration as described above relies on prior knowledge of the vesicle radius distribution. It also relies on the assumption that the vesicular neurotransmitter concentration is constant. For this reason, there is inherently a lack of information regarding the distribution of vesicular DA concentration. In this paper, a model is described to approximately quantify the vesicle radius and vesicular neurotransmitter concentration distributions directly from exocytosis data without prior knowledge of the radius distribution, therefore extending the amount of information available from amperometry data. The assumption that the vesicular neurotransmitter concentration is constant is not used. Rather, a concentration distribution is calculated directly from parameters within the data. The model is demonstrated by application to amperometric exocytosis data obtained at the cell body of the giant dopamine neuron of the pond snail *P. corneus*.

2. Experimental

2.1. Electrodes and voltammetric procedures

Carbon fiber working electrodes were prepared from 10-μm diameter carbon fibers sealed in glass capillaries (Kelly and Wightman, 1986). The sensing tip of the electrode was exposed by cleaving with a surgical blade. The reference electrode was a Ag/AgCl pellet electrode (RC1, World Precision Instruments, Sarasota, FL). Constant potential amperometry was performed with a commercial potentiostat (EI-400, Ensman Instrumentation, Bloomington, IN) in the two-electrode mode. The applied potential was 700 mV. The analog data was output to an A/D converter (Labmaster, Scientific So-

lutions, Solon, OH) interfaced to a 486DX33 personal computer (Gateway 2000, N. Sioux City, SD). All data were digitized at 2 kHz and filtered with a 500-Hz two-pole low pass Bessel filter. Data were analyzed as per Chen et al. (1995). All values are reported as mean ± standard error of the mean unless otherwise stated.

2.2. Cell procedures

P. corneus were obtained from NASCO (Fort Atkinson, WI) and were maintained in aquaria at room temperature until used. The snails were dissected under a snail Ringer solution (39.5 mM NaCl, 1.3 mM KCl, 4.5 mM $CaCl_2$ and 6.9 mM $NaHCO_3$) adjusted to pH 7.4. The dissection procedure and the identification of the dopamine containing neuron were described previously (Osborne et al., 1975; Lichtensteiger et al., 1979; Steiner and Felix, 1987; Chen and Ewing, 1995; Chen et al., 1995). Snail shells were broken and removed before snails were pinned with the ventral side uppermost in a wax-filled Petri dish. The skin of the head part was cut open to reveal the brain. The ganglia ring was pinned at the connective tissue to the wax with 7–10 pins to extend the brain and expose individual cells. The outer connective tissue surrounding the brain was transparent and the orange-colored neurons could be seen beneath using a binocular microscope (70 × magnification). The outer connective tissue was removed from the surface of the pedal ganglion by a home-made fine pin with a 90-degree hook. The dopamine neuron is usually the largest cell (75–150 μm in diameter) in the left pedal ganglion and is easily identified by its specific location close to the statocyst (Marsden and Kerkut, 1970; Pentreath et al., 1974; Osborne et al., 1975). Experiments were performed immediately after dissection.

The Petri dish containing the dissected snail was placed on the stage of a stereomicroscope (Nikon, Tokyo, Japan). A working electrode was positioned over the top of the cell body of the dopamine containing neuron with a three-dimensional micromanipulator (Mertzhauser, Zeiss, Germany). The electrode was manipulated so that it lightly touched the center of the cell body. Release of dopamine from the cell body of the dopamine neuron was induced through short-duration (2–6 s) local applications of 1 M KCl solution prepared in the snail Ringer solution (this corresponded to injections of 170–530 nl). All stimulation solutions were delivered by glass micropipettes controlled by a two-channel pressure application device (Picospritzer, General Valve, Fairfield, NJ). Typical tip dimensions of micropipettes were 10 μm. They were positioned with a micropositioner (Medical Systems, Greenvale, NY) to a desired distance (5–20 μm) from the cell body. Experiments were carried out at room temperature.

2.3. Reagents

Electrode response was tested prior to each experiment in a standard dopamine (DA) solution. Dopamine was obtained from Sigma (St Louis, MO) and was used as received. Dopamine solutions were deoxygenated for 20 min prior to experiments and a blanket of nitrogen was then maintained over the solution. All solutions were prepared with doubly distilled water.

3. Results and discussion

3.1. Exocytosis

A representative amperometric current–time trace from an exocytosis experiment at the cell body of the GDC of *P. corneus* is shown in Fig. 1A. Fig. 1B is an expansion of the time scale that shows seven individual current transients representing the release of seven dopamine containing vesicles. Trapezoidal integration of the current–time trace yields the charge passed at the electrode surface. From Eq. (1), the number of moles of dopamine detected per event is calculated. Combining data from 16 cells, a histogram of vesicular dopamine content can be created and is shown in Fig. 1C.

As several studies of vesicle radius have shown a near Gaussian distribution, plotting the frequency vs. the cube root of the amount of dopamine in each vesicle provides a near Gaussian distribution (Fig. 1D) (Finnegan et al., 1996). This suggests that vesicle size is a key parameter in determining the amount released for each exocytosis event if the concentration of dopamine in every vesicle is equivalent. However, the imperfect Gaussian distributions shown in Fig. 1D suggest the vesicular dopamine concentration could vary across different vesicles. Thus the assumption that vesicular dopamine concentration is constant is an oversimplification.

3.2. Model of exocytosis

In one textbook explanation, exocytosis is depicted as a seven-step process (Kandel et al., 1991). Two of the steps that can be manifested in amperometry data are the formation of a fusion pore and its subsequent dilation. There are several reports of different fusion pore processes occurring before the vesicular contents are ultimately released (Chow et al., 1992; Alvarez de Toledo et al., 1993; Jankowski et al., 1993; Bruns and Jahn, 1995). The majority of the release events, however, ultimately lead to dilation of the fusion pore resulting in release of the contents of the vesicle. We have developed a model of exocytosis that can be used to analyze amperometric current transients resulting from the fusion pore opening and then dilating.

The model is employed to calculate the vesicular dopamine concentration and vesicle radius distributions without assuming that the vesicular concentration is constant. A simplified pictorial representation of exocytosis in Fig. 2A depicts several vesicles at different stages of exocytosis. The vesicle marked as (a) is a vesicle inside the cell that is not yet in contact with the cell membrane. Vesicle (a) simply indicates that there

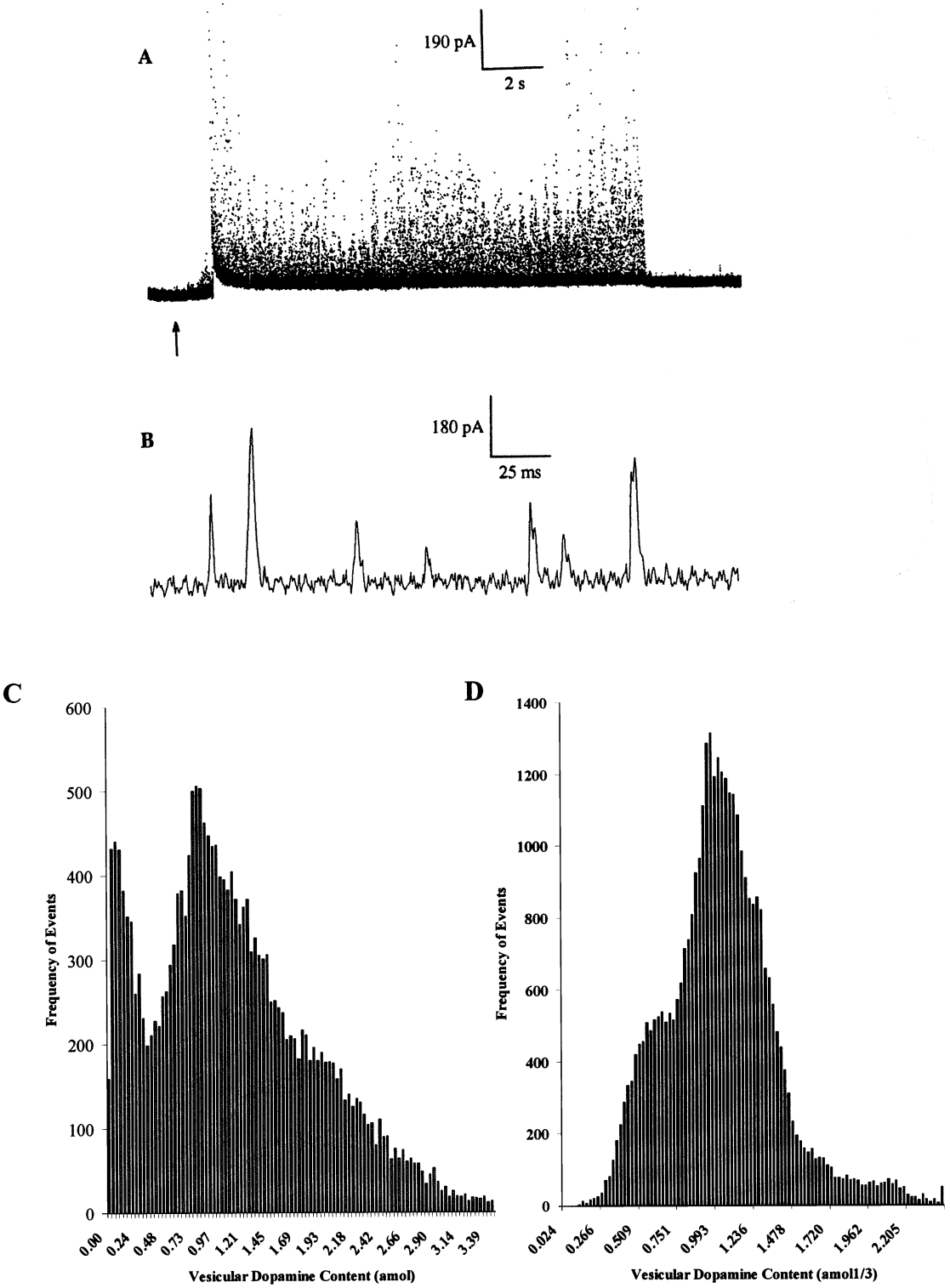

Fig. 1. Amperometric exocytosis data as obtained from the cell body of the giant dopamine neuron of *P. corneus*. (A) Representative current trace from a single stimulation. (B) Expansion of the time axis for seven sequential current transients from (A). (C) Histogram of vesicular content for 16 501 measured release events. (D) Cube root of vesicle content histogram for the same data as in (C).

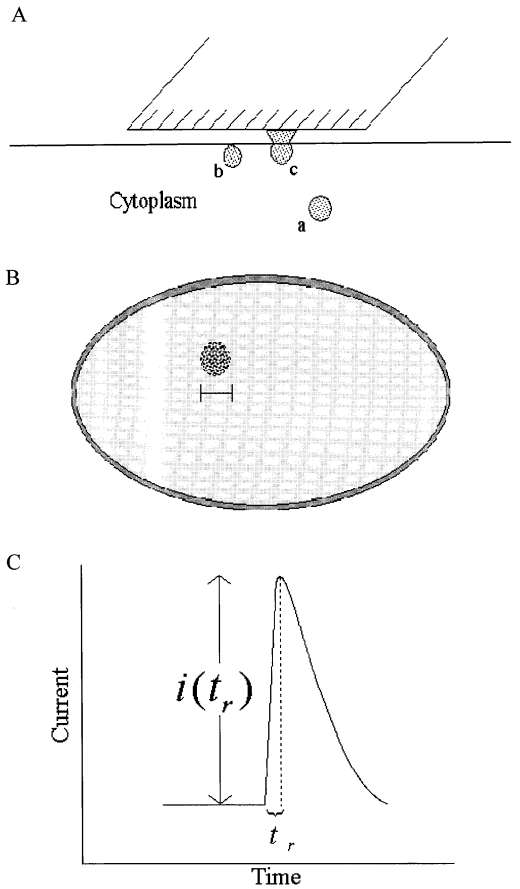

Fig. 2. Model of exocytosis. This is not to scale. To adequately depict the vesicle geometries we have made the vesicle size in (A) and (B) much larger than the normal 1/1500 of the electrode diameter. (A) A carbon fiber microelectrode is manipulated up to a section of the surface of the cell and held at 0.7 V to detect dopamine (shaded area) released from vesicles that are inside the cell. Vesicle 'a' depicts a vesicle that is inside the cell and may or may not be released under the electrode. A release event that does not occur directly underneath the electrode is not detected. Vesicle 'b' depicts a vesicle that has come in contact with the inner cell membrane and has formed a fusion pore. Vesicle 'c' depicts a vesicle that has a dilated fusion pore, which allows dopamine inside the vesicle to diffuse to the electrode surface. The released contents of vesicle 'c' exhibit some diffusional spreading but the area that it affects on the electrode surface is approximately the cross-sectional area of the vesicle. (B) Depiction of the surface of the electrode in (A) when transmitter released from vesicle 'c' has contacted it. The electroactive area of the electrode is approximately defined by the radius of each vesicle detected. The scale bar therefore represents the diameter of the vesicle as it influences the electrode. (C) The current transient shown represents the oxidative current transient that results from the detection of a release event such as 'c' in (A). The rise time (t_r) is the time it takes the signal to go from baseline to maximum. The maximum of the current transient is defined as $i(t_r)$.

are vesicles in the cell that are not released or are released at sites that are not within the spatial resolution of the electrode. The vesicle marked (b) is in contact with the cell membrane and a fusion pore is being formed. This vesicle is important because some or all vesicular contents might escape before the pore is completely open or it might simply close after opening. The vesicle marked (c) is in the process of releasing its contents through the dilated fusion pore. Since the electrode is in contact with the cell, the released contents of vesicle (c) are oxidized rapidly. Rapid oxidation and limited space for diffusion force the oxidation reaction to occur at an area of the electrode approximately defined by the diameter of the vesicle. This geometry is depicted in the end-on view of the electrode shown in Fig. 2B. Using the approximation of geometric conservation, the size of the vesicles has been calculated as described below. It is a release event such as vesicle (c) that results in the experimental current transients (Fig. 1A,B) such as the one simulated in Fig. 2C.

3.3. Electrochemical response

The analytical solution to the electrochemical problem of a concentration packet diffusing from a hemispherical or planar origin to an electrode surface where the contents are oxidized is not known. Therefore, an approximation has been made using the Cottrell equation (Bard and Faulkner, 1980).

$$i(t) = \frac{nFAD^{1/2}C}{\pi^{1/2}t^{1/2}} \quad (2)$$

The Cottrell equation describes the time-dependent current, $i(t)$, at any time, t, for a large potential step past the redox potential of the analyte of interest at a planar electrode of area, A, where D is the diffusion coefficient of the substance being oxidized, and C is the concentration of the reacting species. Conversely, when monitoring exocytosis, a time-dependent change in current occurs following a change in concentration of released transmitter at the electrode.

In principle, a concentration step should be equivalent to a potential step experiment and the small size of the event should lead to microelectrode-like behavior in a thin layer cell. Thus, the maximum of each current transient ($i(t)$, Fig. 2C) can be approximated as a point on the time-dependent current decay of a chronoamperogram (described by Eq. (2)), at time, t (the rise time of a transient as defined in Fig. 2C). In other words, the maximum of the exocytotic current transient intersects with a superimposed chronoamperogram on the time-dependent current decay at time, t. Given this assumption, Eq. (2) provides a reasonable estimate of the time-dependent current decay of transients from amperometric detection of vesicular DA release such as those in Fig. 1A. In fact, if i vs. $t^{1/2}$ is plotted, a correlation of 0.9 is obtained (data not shown). Therefore, the variables C and A in Eq. (2) define the vesicular DA concentration and the size of each vesicle, respectively. Equations to evaluate the relative vesicular DA concentration and vesicle radius can thus be derived as shown below.

3.4. Equations for radius and concentration

To calculate concentration by Eq. (2), the electroactive area of the electrode, A, must be known. The second assumption important to this model, illustrated in Fig. 2B, is that the released contents of a vesicle are detected on the surface of the electrode as a circular area defined by $4\pi r_{ves}^2$, where r_{ves} is the radius of each detected vesicle (note, as the spherical area of the vesicle fuses with the cell membrane, it becomes a disk with radius $2r_{ves}$). Although microelectrodes are used in this study, the electrode is large compared to the geometry of the vesicular contents reaching its surface. Therefore, A can be considered an effective electroactive area due to the geometry of the released vesicular contents. This study uses 10-μm diameter carbon fiber electrodes vs. a vesicle diameter on the order of 50–250 nm (Pentreath and Cottrell, 1974; Pentreath et al., 1974; Osborne et al., 1975; Pentreath and Berry, 1975). In the most unfavorable case, if the vesicle depicted in Fig. 2B is 250 nm in diameter, the electrode area is 800-fold larger than the area defined by r_{ves}. Also, since the electrode is directly on top of the cell, there is minimal diffusional spreading of the released molecules. Therefore, the area of the detection zone is approximately the quantity A in Eq. (2).

By applying the assumptions given above, and using the experimentally measurable parameters ($i(t_r)$ and t_r), Eq. (2) can be rewritten to give

$$i(t_r) = \frac{nF4\pi r_{ves}^2 D^{1/2} C_{DA}}{\pi^{1/2} t_r^{1/2}} \quad (3)$$

where C_{DA} is the concentration of dopamine inside the vesicle. Eq. (3) has two unknowns: C_{DA} and r_{ves}. Rearranging Eq. (1) to obtain C_{DA}, and defining this concentration in terms of moles per volume of the spherical vesicle ($\frac{4}{3}\pi r_{ves}^3$), Eq. (4) is obtained.

$$C_{DA} = \frac{3Q}{4\pi nF r_{ves}^3} \quad (4)$$

The concentration is thus expressed in terms of the measurable parameter, Q, and r_{ves}. Combining Eqs. (3) and (4), an expression for r_{ves} is obtained:

$$r_{ves} = \frac{3D^{1/2}}{5\pi^{1/2}} \times \frac{Q}{t_r^{1/2} i(t_r)} \quad (5)$$

This analysis provides two equations (Eqs. (4) and (5)) and two unknowns (r_{ves} and C_{DA}), and can be used to calculate distributions of the two variables.

3.5. Radius distribution

The average vesicle radius for 16 501 detected release events as calculated from Eq. (5) is 630 ± 2 nm. Clearly, this model is a gross oversimplification and this number is not accurate. However, the important aspect of this work is that relative distributions can be calculated. By sorting the values of radius into equally spaced bins and normalizing to the largest value of r_{ves}, a histogram of vesicle radius can be constructed (Fig. 3). The vesicle radius histogram reveals two distinct distributions. A narrow distribution of small vesicles is centered at an x-axis value of 3% and a broad distribution of larger vesicles is centered at an x-axis value of 35%.

Ultrastructural studies of *P. corneus* have shown that there is a wide distribution of vesicle size in the giant dopamine neuron (50–250 nm) (Pentreath and Cottrell, 1974; Pentreath et al., 1974; Osborne et al., 1975; Pentreath and Berry, 1975). Those studies, however, do not point out that specific distributions of vesicle size occur, possibly because of the limited spatial resolution of the technique (0.1 μm) (Pentreath and Berry, 1975). Although the ultrastructural studies do not suggest multiple distributions of vesicle size, it has been shown more recently that multiple size distributions of vesicles exist in neurons (Boone and Aldes, 1984; King et al., 1984; Chazal and Ralston, 1987; Buffa et al., 1988; Fox, 1988; Novotny, 1988; Fox et al., 1989; May and Warren, 1993). In particular, it has been suggested that there are at least two classes of vesicles based on vesicle size in *P. corneus* (Chen and Ewing, 1995). The calculations for radius in this work support the hypothesis by the bimodal radius distribution shown in Fig. 3.

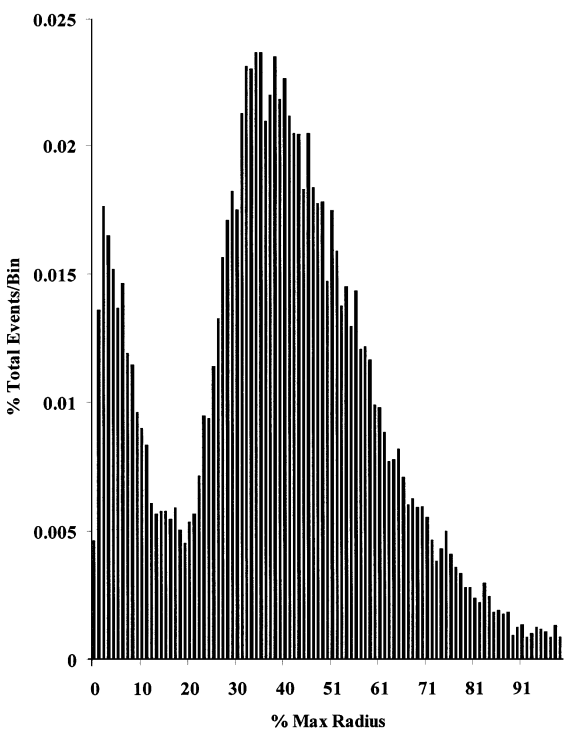

Fig. 3. A 100-bin histogram (8 nm per bin) of the vesicle radius was calculated by Eq. (5) for the same data as in Fig. 1. The x-axis is normalized to the maximum value for radius.

One possible explanation for two vesicle radius distributions is that they could represent large dense core vesicles (LDCV) and small synaptic vesicles (SSV) released from the cell body. Bruns and Jahn (1995) report electrochemical detection of multiple classes of vesicles from the leech serotonin neuron and that the two vesicle amount distributions correspond to SSV and LDCV. Electron microscopy experiments have shown that leech SSVs are known to have a tight size distribution with a diameter of 37.8 ± 0.7 nm, whereas the LDCVs have a wide range of values from 55 to 150 nm in diameter (Henderson et al., 1983). The vesicle size distributions reported for the leech are similar to those presented here for *P. corneus* in that there is a narrow distribution of small vesicles and a broad distribution of larger vesicles. Although the quantitative aspect of this model is approximate, the results presented here are consistent with the limited data in the literature suggesting two distinct sizes of vesicle radius in these cells.

3.6. Vesicular dopamine concentration

This model allows a histogram of the vesicular dopamine concentration to be calculated. The range of values for concentration covered more than five orders of magnitude. In order to view all of the data on a single 100-bin histogram, a logarithmic histogram has been constructed (Fig. 4). This histogram, like Fig. 3, has been normalized to the largest value of concentration. The logarithmic scaling compresses the data into a range that can be plotted on a 100-bin histogram. It appears that there might be a shoulder on the right-hand side of the main distribution of vesicular dopamine concentration. It is unclear if the shoulder is significant or if it is an anomaly of the logarithmic binning. It is apparent from Fig. 4 that the concentration distribution is skewed toward larger concentrations. The breadth of the distribution makes interpretation of the data difficult. However, it appears that the two distributions shown in Fig. 3 are represented by a range of concentration, not a single value.

The mean vesicular DA concentration for all 16 501 detected events by Eq. (4) is 0.070 ± 0.003 mol/l. Since the range of values is so enormous, the median concentration (1.2 mM) is more descriptive of the distribution. This median value is low compared to vesicular catecholamine concentration of adrenal cells (0.15 M; Finnegan et al., 1996) and the vesicular serotonin concentration of the leech (0.270 M; Bruns and Jahn, 1995). The concentration values reported for these cells, however, are based on the mean values of both vesicle amount and vesicle radius measured by electron microscopy. As there is no current method to directly evaluate concentrations of transmitter in single vesicles, the use of mean values could be misleading. Also, there is no indication of the distribution of concentration.

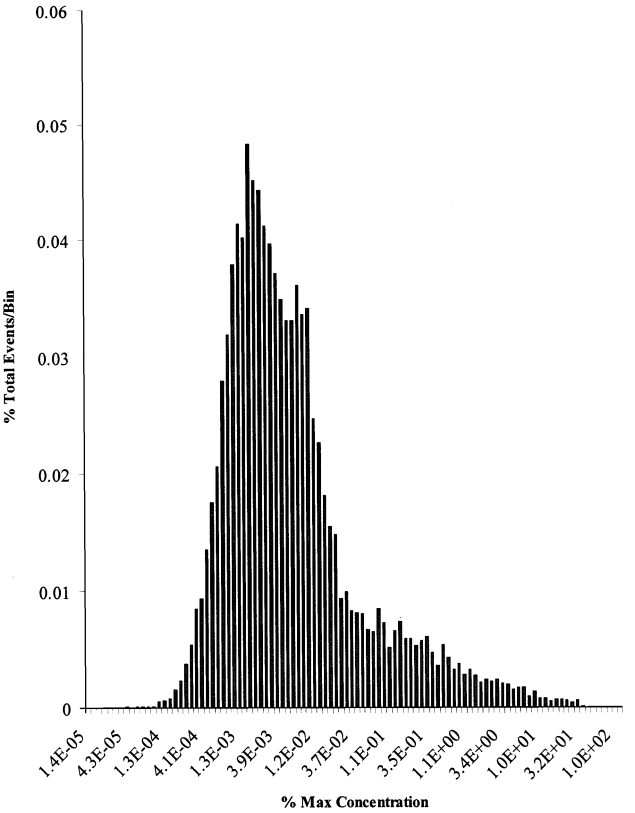

Fig. 4. A 100-bin logarithmic histogram (0.002 log units per bin) of the vesicular dopamine concentration. Vesicular dopamine concentration was calculated by Eq. (4) for the same data as in Fig. 1. The values for concentration range over more than five orders of magnitude and cannot be presented on a traditional histogram. By taking the base 10 logarithm of each of the values for concentration, a 100-bin histogram can be constructed. The x-axis has been normalized to the maximum concentration value.

3.7. Diffusion coefficient

One important aspect of Eq. (5) is that there is a square root dependence of radius on D so a 20-fold decrease in D will result in about a 4.5-fold decrease in radius and almost a 100-fold increase in concentration. In the work presented here, the value of D used is that of catecholamines in aqueous solution (6×10^{-6} cm^2/s) (Gerhardt and Adams, 1982). If a value of 3×10^{-7} cm^2/s is employed for D as taken from Chow et al. (1992) the average vesicle radius is 142.6 ± 0.6 nm and the median vesicular DA concentration is 100 mM. The dependence of radius on D therefore restricts absolute quantitation as it is difficult to obtain accurate values of D in biological systems. However, other than an x-axis shift, the shape of the distributions is expected to remain the same. Thus the model presented here is clearly useful for comparisons of vesicle radius and dopamine concentration distributions between exocytosis events and different cells.

3.8. Fusion pore

Formation of the fusion pore and its subsequent dilation resulting in exocytosis can be studied by amperometry (Chow et al., 1992; Schroeder et al., 1996). These two processes are important to this work and are highlighted in Fig. 2A by vesicles (b) and (c). Although it is not apparent in these data (Fig. 1A,B), there might be events with a pre-spike feature preceding some of the current transients. The data presented here, however, represent release events that result from dilation of the fusion pore to allow the contents to be released and detected as current transients such as those in Fig. 1. It is possible that some of the events are a result of the vesicular contents diffusing through an undilated fusion pore as suggested for SSV by Bruns and Jahn (1995). Under those circumstances, the model presented here would represent the fusion pore radius not the vesicle radius. Finally, if a fusion pore opens and closes in a rapid flicker, it is expected to result in current transients that are extremely rapid compared to those shown in Fig. 1 so there is no effect on the model presented here.

4. Conclusion

The model reported here provides a basis for calculating relative distributions of transmitter concentration in vesicles and vesicle radius. This work provides evidence that vesicles in the *P. corneus* neuron have two distributions of radius and a wide range of dopamine concentration. Thus, previous models assuming a uniform concentration of transmitter in vesicles may have been oversimplified.

As noted throughout this text, the values of vesicular radius and DA concentration are approximate and the value of D has a large effect on the calculated values. An exact value for D would obviously increase the quantitative accuracy of this model. Solving the current–time equations for the problem is another possible improvement for the quantitative aspect of this model. Regardless of the exact quantitation, however, the shape of the distributions remains the same. Since the exact quantitation does not affect the distributions, this model is useful for determining relative changes in vesicle size or neurotransmitter concentration due to pharmacological or molecular biological challenges.

Acknowledgements

The authors thank Don Cannon for his help in the preparation of this manuscript. This work was supported by the National Institutes of Health.

References

Alvarez de Toledo G, Fernández-Chacón R, Fernández JM. Release of secretory products during transient vesicle fusion. Nature 1993;363:554–8.

Bard AJ, Faulkner LR. Electrochemical Methods: Fundamentals and Applications. New York: Wiley, 1980:142–4.

Boone TB, Aldes LD. Synaptology of the hypoglossal nucleus in the rat. Exp Brain Res 1984;57:22–32.

Bruns D, Jahn R. Real time measurement of transmitter release from single synaptic vesicles. Nature 1995;377:62–5.

Buffa R, Rindi G, Sessa F, Gini A, Capella C, Jahn R, Navone F, Camilli PD, Solcia E. Synaptophysin immunoreactivity and small clear vesicles in neuroendocrine cells and related tumors. Mol Cell Probes 1988;2:367–81.

Chazal G, Ralston HJ III. Serotonin-containing structures in the nucleus raphe dorsalis of the cat: an ultrastructural analysis of dendrites, presynaptic dendrites, and axon terminals. J Comp Neurol 1987;259:317–29.

Chen G, Ewing AG. Multiple classes of catecholamine vesicles observed during exocytosis from the *Planorbis* cell body. Brain Res 1995;701:167–74.

Chen G, Gavin PF, Luo G, Ewing AG. Observation and quantitation of exocytosis from the cell body of a fully developed neuron in *Planorbis corneus*. J Neurosci 1995;15:7747–55.

Chen G, Gutman DA, Zerby SE, Ewing AG. Electrochemical monitoring of bursting exocytosis events from the giant dopamine neuron of *Planorbis corneus*. Brain Res 1996;733:119–24.

Chen TK, Luo G, Ewing AG. Amperometric monitoring of stimulated catecholamine release from rat pheochromocytoma (PC 12) cells at the zeptomole level. Anal Chem 1994;66:3031–5.

Chow RH, von Ruden L, Neher E. Delay in vesicle fusion revealed by electrochemical monitoring of single secretory events in adrenal chromaffin cells. Nature 1992;356:60–3.

Clark RA, Ewing AG. Quantitative measurements of released amines from individual exocytosis events. Mol Neurobiol 1997;15:1–16.

Coupland RE. Determining sized and distributions of sizes of spherical bodies such as chromaffin granules in tissue sections. Nature 1968;217:384–8.

Finnegan JM, Pihel K, Cahill P, Huang L, Zerby SE, Ewing AG, Kennedy RT, Wightman RM. Vesicular quantal size measured by amperometry at chromaffin, mast, pheochromocytoma, and pancreatic β-cells. J Neurochem 1996;66:1914–23.

Fox GQ. A morphometric analysis of synaptic vesicle distributions. Brain Res 1988;474:103–17.

Fox GQ, Kotting D, Dowe GHC. A morphometric analysis of Torpedo synaptic vesicles isolated by iso-osmotic sucrose gradient separation. Brain Res 1989;498:279–88.

Gerhardt G, Adams RN. Determination of diffusion coefficients by flow injection analysis. Anal Chem 1982;54:2618–20.

Henderson LP, Kuffler DP, Nicholls JG, Zhang R-J. Structural and functional analysis of synaptic transmission between identified leech neurons in culture. J Physiol 1983;340:347–358.

Jankowski JA, Schroeder TJ, Ciolkowski EL, Wightman RM. Temporal characteristics of quantal secretion from adrenal medullary cells. J Biol Chem 1993;268:14694–700.

Kandel ER, Schwartz JH, Jessel TM. Principles of Neuroscience, 3rd edn. Norwalk, CT: Appleton and Lange, 1991:230–1.

Kelly RS, Wightman RM. Bevelled carbon-fiber ultramicroelectrodes. Anal Chim Acta 1986;187:79–87.

Kennedy RT, Huang L, Atkinson MA, Dush P. Amperometric monitoring of chemical secretions from individual pancreatic β-cells. Anal Chem 1993;65:1882–7.

King JS, Ho RH, Burry RW. The distribution and synaptic organization of serotonergic elements in the inferior olivary complex of the opossum. J Comp Neurol 1984;227:357–68.

Larsson LI, Sundler F, Hakanson R. Pancreatic polypeptide—a postulated new hormone: identification of its cellular storage site by light and electron microscopic immunocytochemistry. Diabetologia 1976;12:211–26.

Leszczyszyn DJ, Jankowski JA, Viveros OH, Diliberto EJ Jr, Near JA, Wightman RM. Nicotinic receptor-mediated catecholamine secretion from individual chromaffin cells. Chemical evidence for exocytosis. J Biol Chem 1990;265:14736–7.

Leszczyszyn DJ, Jankowski JA, Viveros OH, Diliberto EJ, Near JA, Wightman RM. Secretion of catecholamines from individual adrenal medullary chromaffin cells. J Neurochem 1991;56:1855–63.

Lichtensteiger W, Felix D, Hefti F. Spike activity and histofluorescence correlated in the giant dopamine neuron of *Planorbis corneus*. Brain Res 1979;170:231–45.

Marsden C, Kerkut GA. The occurrence of monoamine in *Planorbis corneus*: a fluorescence microscopic and microspectrometric study. Comp Gen Pharmacol 1970;1:101–16.

May PJ, Warren SJ. Ultrastructure of the macaque ciliary ganglion. Neurocytology 1993;22:1073–95.

Novotny GEK. Ultrastructural analysis of lymph node innervation in the rat. Acta Anat 1988;133:57–61.

Osborne NN, Priggemeier E, Neuhoff V. Dopamine metabolism in characterized neurons of *Planorbis corneus*. Brain Res 1975;90:261–71.

Pentreath VW, Berry MS. Ultrastructure of the terminals of an identified dopamine-containing neurone marked by intracellular injection of radioactive dopamine. J Neurocytol 1975;4:249–60.

Pentreath VW, Cottrell GA. Ultrastructure of a giant dopamine-containing neurone in *Planorbis corneus*. Experientia 1974;30:293–4.

Pentreath VW, Berry MS, Cottrell GA. Anatomy of the giant dopamine-containing neuron in the left pedal ganglion of *Planorbis corneus*. Cell Tissue Res 1974;151:369–84.

Pihel K, Hsieh S, Jorgenson JW, Wightman RM. Electrochemical detection of histamine and 5-hydroxytryptamine at isolated mast cells. Anal Chem 1995;67:4514–21.

Schroeder TJ, Borges R, Finnegan JM, Pihel K, Amatore C, Wightman RM. Temporally resolved, independent stages of individual exocytotic secretion events. Biophys J 1996;70:1061–8.

Schubert D, LaCorbiere M, Klier FG, Steinbach JH. The modulation of synthesis by steroid hormones and insulin. Brain Res 1980;190:67–79.

Steiner FA, Felix D. Effects of hypothalamic releasing hormones and biogenic amines on identified neurons in the circumoesophageal ganglia of the water snail. Comp Biochem Physiol 1987;92C:301–7.

Wightman RM, Jankowski JA, Kennedy RT, Kawagoe KT, Schroeder TJ, Leszczyszyn DJ, Near JA, Diliberto EJ Jr, Viveros OH. Temporally resolved catecholamine spikes correspond to single vesicle release from individual chromaffin cells. Proc Natl Acad Sci USA 1991;88:10754–8.

Wightman RM, Schroeder TJ, Finnegan JM, Ciolkowski EL, Pihel K. Time course of release of catecholamines from individual vesicles during exocytosis at adrenal medullary cells. Biophys J 1995;68:383–90.

Zerby SE, Ewing AG. The latency of exocytosis varies with the mechanism of stimulated release in PC12 cells. J Neurochem 1996;66:651–7.

Zhou R, Luo G, Ewing AG. Direct observation of the effect of autoreceptors on stimulated release of catecholamines from adrenal cells. J Neurosci 1994;14:2402–7.

Zhou Z, Misler S. Amperometric detection of stimulus-induced quantal release of catecholamines from cultured superior cervical ganglion neurons. Proc Natl Acad Sci USA 1995;92:6938–42.